IEEE Access
Multidisciplinary | Rapid Review | Open Access Journal

Received August 17, 2021, accepted September 2, 2021, date of publication September 6, 2021,
date of current version September 15, 2021.

Digital Object Identifier 10.1109/ACCESS.2021.3110582

System Based on Compact mmWave Radar and Natural Body Movement for Assisting Visually Impaired People

HUMBERTO FERNÁNDEZ ÁLVAREZ, GUILLERMO ÁLVAREZ-NARCIANDI, FERNANDO LAS-HERAS, (Senior Member, IEEE), AND JAIME LAVIADA
Department of Electrical Engineering, Universidad de Oviedo, 33203 Gijón, Spain

Corresponding author: Jaime Laviada (laviadajaime@uniovi.es)

This work was supported in part by the Ministerio de Ciencia, Innovación y Universidades, Spain Government, under Project MILLIHAND RTI2018-095825-B-I00, and in part by the Gobierno del Principado de Asturias and European Union (FEDER) under Project GRUPIN-IDI-2018-000191.

ABSTRACT The aim of this paper is to show how compact mmWave radar systems, attached to a person, can take advantage of their movements, in order to significantly improve the image resolution by means of synthetic aperture radar (SAR) techniques. Thus, high resolution imaging becomes possible even with tiny on-chip systems, opening up a horizon of possibilities to assist visually impaired people. The approach is illustrated for movements in terms of arm swings. For this purpose, it is firstly shown that the information from an inertial measurement unit (IMU) can be used to provide a trajectory estimation, which is enough to apply synthetic aperture radar processing. As a consequence, the resolution of the radar is greatly improved when compared with that achieved considering a single position. In order to avoid the continuously growing position error, commonly observed in dead-reckoning systems relying just on IMU, zero velocity updates (ZUPT) will be systematically applied. For doing so, two different zero velocity detectors (ZVD) are considered, one based on acceleration data and other on velocity estimation. Although the positioning information is extracted from the IMU, demonstrating the enhanced obstacle detection capabilities obtained with this approach, other sensors that can be carried by a person and that are capable of providing trajectory estimations to combine measurements acquired with compact mmWave radars could have been used. The system is tested using different targets and a good performance comparable to the one achieved by using a high accuracy reference positioning system is attained. The compactness of the system enables the possibility of using it as a wearable device, e.g., attached to the wrist. This shows that an IMU is enough for tracking relatively simple movements, though more complex positioning systems can be used for more general actions.

INDEX TERMS Freehand imaging, visually impaired, inertial measurement unit, mmWave radar, synthetic aperture radar (SAR), wrist mounted imager, zero velocity detectors (ZVD).

I. INTRODUCTION

Radar technology has been widely used to detect the distance, angular position and/or velocity of objects, such as ships, vehicles or aircrafts [1]. Its working principle is based on the reflection of radio waves on them and the application of different phenomena, such as wave propagation, Doppler effect and phase of arrival [2]. This technology not only enables the detection of visible objects, but also concealed or covered ones [3], as electromagnetic waves can propagate through several materials.

Thanks to the advent of new technologies, such as the autonomous vehicles and advanced driver-assistance systems (ADAS), radar technology has experimented a great technological leap [4] and now, compact mmWave radars are available at an affordable price [5]. Moreover, the technology has been greatly compacted, enabling tiny radar-on-chip systems [6], which are excellent candidates for the development of new compact and wearable devices. In addition, mmWaves are robust to harsh environmental conditions [7] and exhibit a

The associate editor coordinating the review of this manuscript and approving it for publication was Davide Comite.

This work is licensed under a Creative Commons Attribution 4.0 License. For more information, see https://creativecommons.org/licenses/by/4.0/

wide range of coverage [8], which outperforms the behavior of other systems, such as the ones based on depth-cameras [9]. Besides, radar signals can pass through clothes, so radar devices do not need to be exposed and can be covered by garments. Finally, they are also able to work under low visibility conditions (fog, smoke, etc.) [10].

Due to the previous features, mmWave radar signals are excellent candidates to assist visually impaired people in their everyday life, aiming at replacing or complementing the traditional aids, such as guide dogs or white canes, which just provide limited information. Recently, new electronic travel aids (ETAs) devices [11] have been developed to help impaired persons to detect objects and warn them by means of sounds and vibrations [12]–[14]. Other systems are based on the fusion of data provided by depth-cameras and mmWave radars, aiming at compensating each sensor drawbacks [15], [16]. In this context, depth-cameras are sensitive to the light and their range resolution is limited. Therefore, they cannot compensate the limited cross-range resolution of radars in a large variety of situations. In addition, most of the proposed systems are based on detecting large objects.

Consequently, radar imaging techniques seem to be a promising solution to circumvent the previous issues and to extract additional information from targets. In [17], a radar with a beam steering antenna is developed to be placed on a person head to create an image of the surrounding environment. However, both a mechanical set-up and the design of a complex antenna are required to cover enough area.

In general, the resolution of a radar system depends on its electrical size. The larger the electrical size, the better the resolution. However, large size devices are not convenient for wearable systems. In this context, synthetic aperture radar (SAR) techniques are of great relevance to improve the *cross-range resolution* and accurately determine the location of targets [18]. This technique involves the movement of an antenna along certain path [19]. Consequently, one can take advantage of the *human motion* and get the required information, to extract an electromagnetic image of the surrounding environment. At this point, it should be remarked that not only the radar information, but also its position and, thus, their antenna locations, is required to create the electromagnetic image.

The positioning information can be obtained using different systems such as optical positioning systems [20], RFID tags [21], GPS information [22], other sensor networks [23] or the combination of different positioning systems [24]. However, most of these systems are just suitable for either indoor or outdoor environments and the majority of them involve the deployment of other sensors in the tracking environment. In addition, specialized devices, devoted to tracking, are slowly becoming available, allowing compact and reliable tracking with enough accuracy to enable mmWave SAR [25].

One of the most extended sensors with tracking capabilities are the inertial measurement units (IMUs). These sensors usually consist of tri-axials gyroscopes and accelerometers. Modern or hybrid IMUs, also known as MARG (magnetic, angular, rate and gravity), incorporate a tri-axial magnetometer too [26]. Both devices have been widely used for orientation and position estimation, enabling a mature technology, which can be greatly miniaturized.

To achieve orientation estimation, the angular rate provided by the gyroscope has to be integrated. However, this integration introduces a drift that it is commonly compensated using different algorithms based on the magnetometer and accelerometer data, such as the one proposed by Madgwick [26] or the nonlinear complementary filter of Mahony [27] among others [28]. Using any of these algorithms, a suitable estimation of the orientation can be obtained. A greater problem arises when estimating the position, as it involves a double integration of the acceleration, causing a significant drift in the estimation [29]. Different correction techniques have been used to compensate this error, such as the employment of complementary information from GPS signals, ultrasonic sensors, cameras or other sensors [30]. However, most of these techniques are only suitable for either indoor or outdoor environments. Other correction methods have been introduced in the literature, such as the Zero Angular Rate Update (ZARU), Magnetic Angular Rate Update (MARU) or Heuristic Drift Reduction (HDR). Nonetheless, they require different conditions to be met that are usually difficult to detect with handheld devices [31]. The most commonly implemented technique is the correction based on zero velocity updates (ZUPT), which corrects velocity errors on an Extended Kalman Filter (EKF) [32]. A key aspect to apply the previous algorithm is the detection of zero velocity. Using acceleration or gyroscope information or a combination of both, the stance phase can be detected [33], [34]. Although this algorithm works fine when the IMU is tied to the foot, it undergoes difficulties when it is attached to the wrist, as the wrist swing frequency is twice the leg one and, hence, the motionless wrist time during natural walk is much shorter [35].

The main contribution of this paper is the study of the capabilities of a compact radar system complemented by a tracking system, to enable a compact wearable SAR imager with capacity to detect nearby obstacles. In this case, an IMU is used as the tracking system as it is one of the most extended sensors, though not the most reliable one. As a consequence of this fusion, the quality of the obtained images in terms of resolution significantly outperforms that of the images retrieved when a single position is considered. The position information is extracted using improved pedestrian dead reckoning techniques, fast sampling rates and new correction algorithms. Although other alternatives to extract the position information are feasible and they enable direct access to this location data [25], [36], the authors have used an IMU, as it is widely available and enables great compactness, but it should be noticed that the goal of this paper is not to introduce a new method for improving the existing algorithms to extract the position information from an IMU. The remainder of this paper is organized as follows. First, the components of the prototype are described together with the overall flowchart

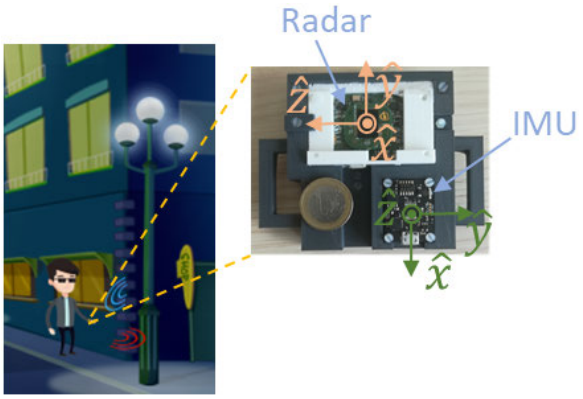

FIGURE 1. Scenario of a visually impaired person walking through the street with the proposed prototype attached to their wrist.

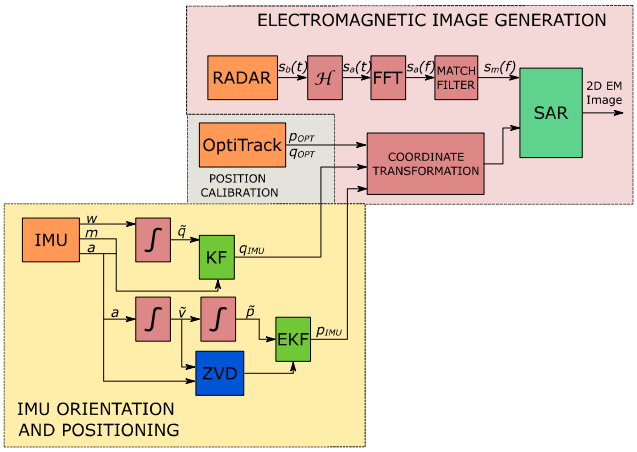

FIGURE 2. Proposed system workflow.

of the system. Next, the tool to track the radar location from the sensor data is developed, which, in our implementation, consists of an algorithm for estimating the position from IMU data, considering two ZUPT algorithms. In the results section several experiments are presented to assess the object detection capabilities under different conditions. Finally, the advantages and disadvantages of the presented approach and future research lines are drawn in Section IV.

II. SYSTEM DESCRIPTION

The prototype used in this work is the one presented in the inset of Figure 1. Although the system relies on off-the-shelf components for easy development and debugging and, consequently, it is not as compact as possible, it is representative of the capabilities that can be achieved by means of the fusion of on-chip radars and IMU data.

On one hand, this prototype includes a frequency modulated continuous mmWave (FMCW) radar module. In particular, the radar-on-chip BGT60TR24B evaluation board manufactured by Infineon [25], [37] has been chosen as it provides a tiny radar with a reduced power consumption, as it was originally developed to be used in mobile phones for gesture detection [38]. On the other hand, the LPMS-CURS2 IMU by LP-Research is used [39], as it comprises a compact board with USB interfacing. Both devices are arranged together using an ad-hoc 3D printed platform.

This prototype is representative of a system that can be easily attached to a person, benefiting from their natural motion to enable high resolution imaging. For example, it can be attached to their wrist, as it is a handy place allowing them to scan and detect objects or obstacles. Moreover, it is an ideal location to prevent collisions with the upper body part, which cannot be avoided using traditional white canes [13].

Figure 2 shows the workflow for data processing. It comprises two main steps: the orientation and positioning extraction and the electromagnetic image generation. There is an additional step, which is called position calibration, that was only introduced for evaluation purposes to assess the performance of the system and will not be in the final product. This latter step enables to measure the accuracy of the proposed system when compared to an accurate reference system based on a commercial motion capture system, consisting of external infrared cameras and a set of markers attached to the prototype.

A. ORIENTATION AND POSITION DETERMINATION

In order to create an electromagnetic (EM) image using synthetic aperture radar techniques, both the orientation and the position of the radar antennas have to be known at each measurement instant[3].

The orientation of the system is computed by applying a Kalman filter (KF) to the IMU data (rotation rate (w), acceleration (a), magnetic field (m)), as it is shown in the yellow background box of Figure 2. This filter properly corrects the gyroscope drift, and hence a suitable information of the orientation is obtained. For convenience, a quaternion (q_{IMU}) representation is employed.

The position of the radar antennas is estimated by a double integration of the measured acceleration provided by the IMU. As it was mentioned, this double integration causes a position drift error that continuously increases. Aiming at correcting this error, a zero velocity detection (ZVD) technique is applied, so that it feeds an extended Kalman filter (EKF), similar to the one proposed in [40], to correct the position deviations. More precisely, the prediction states of the EKF, computed using the inertial navigation equations, are corrected by calculating the predicted error when zero velocity is detected. The latter helps the system to systematically correct its error and avoid the growing drift on the position estimation.

Using the previous procedure, the system can work autonomously and independently from other sensors, being suitable not just in outdoor, but also in indoor environments. The main problem in this stage is the accurate detection of the zero velocity to properly correct the error, as an imprecise correction of the predicted states on the EKF, introduces larger positioning errors than the ones added by the IMU positioning drift.

B. ZERO VELOCITY DETECTION

As it was previously mentioned, the available ZVD algorithms in the literature are suitable when the IMU is tied to the foot, but their accuracy clearly worsens when it is attached to the wrist. However, most applications (such as the ones related with health monitoring) do not require a precise determination of zero velocity, as they just measure steps and the accurate determination of the step stages does not matter on the counting process.

In this article, two different zero velocity detection algorithms based on the movement of the wrist are considered. Figure 3 and 4 show the proposed algorithms workflows. One of them relies on the acceleration and the other on the estimated velocity.

The acceleration based ZVD algorithm comprises a pre-processing stage, in which a coordinate system transformation is applied to get the acceleration in the IMU coordinate system ($a_p(t)$, see Figure 3). Then, an FFT (Fast Fourier Transform) is performed to examine the acceleration harmonics ($a_p(f)$). After an empirical analysis, it was observed that the wrist swinging phase exhibits a predominant harmonic component due to the arm movement (in this paper static swings will be considered). Therefore, in the post-processing stage the noisy higher frequency harmonic components are removed, using a rectangular filtering window ($\Pi(f)$) and then, a smoother signal ($a_{pp}(t)$) is recovered after applying the Inverse Fast Fourier Transform (IFFT), which better represents the arm movement. Finally, a peak/valley finding (PVF) algorithm is implemented, which also ensures that after a peak there is a valley and vice versa, so that just the most likely zero velocity positions, $ZVD_a(t)$, are identified on each swing. For comparison purposes, the $ZVD_a(t)$ is compared to the one obtained using the reference system, $ZVD_o(t)$, in the last image of figure 3 using a binary representation (1 and 0 for either zero velocity detection and non-detection, respectively), noticing slight differences between both.

In the velocity based ZVD, a pre-processing stage, similar to the one conducted in the previous algorithm for transforming the acceleration data to the IMU coordinate system, is applied. Then, the inertial navigation equation given by:

$$\tilde{v}(t) = \tilde{v}_0 + \int_{t_s} a_p(t)dt, \tag{1}$$

wherein $\tilde{v}_0$ is the initial velocity and t_s is the sampling interval, is used to predict the velocity $\tilde{v}(t)$. After that, a post-processing stage is applied, which comprises the application of a high-pass zero-phase digital filter to the estimated velocity data, obtaining $\tilde{v}_{pp}(t)$. Finally, a zero-cross function (ZCF) is used to determine the zero velocity positions ($ZVD_v(t)$). As in the previous case, the $ZVD_v(t)$ is compared with the $ZVD_o(t)$ in Figure 4 obtaining slight discrepancies.

C. ELECTROMAGNETIC IMAGE GENERATION

This module creates the 2D electromagnetic image of the scenario under evaluation. The workflow is shown in the red background part of Figure 2 and it is based on the one described in [3]. As previously discussed, SAR techniques allows to increase the lateral resolution of electromagnetic images. For that purpose, it is necessary to coherently combine the acquired data and, therefore, the position the radar transmitters and receivers must be known.

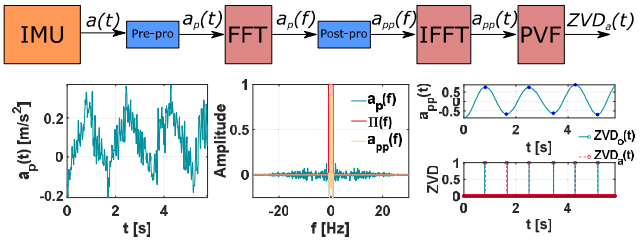

FIGURE 3. Acceleration based ZVD workflows and signals.

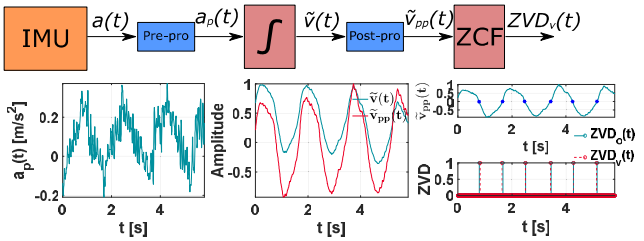

FIGURE 4. Velocity based ZVD workflows and signals.

The employed FMCW radar module performs dechirped-on-receive operations and, considering a point target, at each sampling position, the received signal $s_b(t)$ can be expressed as

$$S_b(t) = e^{j2\pi\left(\frac{BW}{T_s}\tau t + f_c\tau - \frac{BW}{2T_s}\tau^2\right)}, \tag{2}$$

where BW is the bandwidth of the radar module, T_s is the chirp duration, f_c is central frequency and τ is the propagation delay, which is proportional to the distance between the radar transmitter and the target, and from the target to the radar receiver. In case of a distributed target, the received signal can be expressed a superposition of signals according to (2). It should be remarked that the radar module does not provide the complex form of $s_b(t)$, but due to its wideband nature a Hilbert transform (H) can be used to obtain it. The next step is to compensate the extra phase term, which can be approximated for close targets by $f_c\tau$, and perform a range compression applying an FFT:

$$S_c(f) = \mathcal{F}\{s_b(t)e^{-j2\pi f_c\tau}\}, \tag{3}$$

where $\mathcal{F}\cdot$ represents the Fourier transform operator. Finally, the reflectivity, ρ, of each point, r', of the scenario under evaluation, i.e., the value of each pixel of the SAR image, after the *m-th* radar acquisition is computed by means of a *delay-and-sum* algorithm:

$$\rho_{\mathrm{m}}(r') = \sum_{i=1}^{m} s_c\left(r', \frac{BW}{T_s}\tau_m\right) \tag{4}$$

At this point, it should be remarked that, in order to coherently combine radar acquisitions the orientation and position of the radar antennas, which are extracted from the IMU data, following the steps mentioned in section II B, must be known. In addition, a motion capture system (OptiTrack®) is used as reference system. Note that this reference system relies on external cameras and, therefore, it is not useful for a real prototype.

The reference frame of the IMU and that of the reference motion capture system are transformed to refer their position and orientation using the same coordinate system. At this point, it should be highlighted that the position extraction is independently retrieved with each system, i.e., the IMU tracking system can be used without the reference system.

Finally, it is worth mentioning that, though the previous algorithms prevent massive drifting, slight drifting will still exist. Thus, if there is a swing so the radar moves back to the same range of positions, the accumulated positioning error could result in this last swing not producing an accurate coherent combination. Thus, it is prudent to consider coherent combinations for relatively short time frames to prevent potentially destructive interferences due to the position drift. In our implementation, these time frames are defined as the length of an entire swing. Consequently, data acquired during each swing is coherently used to generated an image using SAR techniques. The final image is achieved by non-coherently adding the images from each swing, i.e., the images are added by considering only their amplitude.

In summary, both the orientation and positioning information, as well as the radar signals are used to create the electromagnetic image using a SAR technique.

FIGURE 5. Measurement set-up: (a) sketch and (b) scenario.

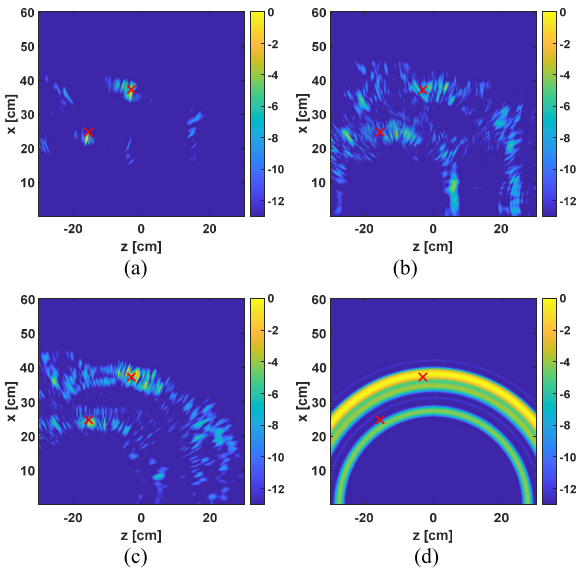

FIGURE 6. Reflectivity images using the acceleration based ZVD information after two swings: (a) reference motion capture system, (b) IMU and (c) IMU + ZUPT. (d) Reflectivity image considering only one radar position.

III. RESULTS AND DISCUSIONS

In order to assess the capability of increasing the resolution of a wearable radar by using the natural motion of the person carrying it, several experiments were conducted with the setup shown in Figure 5. Although the signal processing could be carried out in an embedded system or wirelessly transmitted to another platform (e.g., a smartphone), a conventional computer was used for this purpose to provide a high degree of flexibility enabling to focus on the core of the system (i.e., use of the radar and the IMU). In addition, it enables to capture the data from the reference system to carry out performance evaluations. In order to mimic an arbitrary motion, several swings are performed in front of the targets. Although this is a simplified case, as it does not consider a constant movement, it enables us to assess the capabilities of the system to exploit the natural motion as long as the position can be tracked. Furthermore, all the swings are considered to be carried out through a similar space region as depicted in Figure 5, which is very challenging as drifts in the positioning error can result in destructive interferences if not properly corrected. It is worthy to remark that this SAR-based approach enhances the cross-range resolution and, therefore, if the movement is mostly done along the one direction (e.g., the z-axis), then the resolution enhancement will be achieved along that direction.

The first experiment is devoted to evaluate the performance in case of narrow obstacles. In this case, the target comprises two cylindrical metallic rods of radius 1.3 cm with a distance of 17.7 cm between them. Both rods are placed at different distances from the radar. In the first scanning test, the radar and the information from the positioning systems (both IMU and reference system) are captured in a serial way, so that the update rate is limited by the slowest subsystem. In this case, the positioning updates are faster than the radar ones. Once the data is recorded, the electromagnetic image is generated, following the steps described in section II-C. Three electromagnetic images will be compared. The first one is obtained using the reference positioning system, which will be compared to the obtained ones using just the IMU and the IMU + ZUPT systems.

The results in Figure 6(a, b, c) and 7 show the three mentioned electromagnetic images corresponding to two swings. The only difference between both figures is the employed ZVD technique, which is the acceleration and the velocity based ZVD, respectively. It should be noticed that the chosen

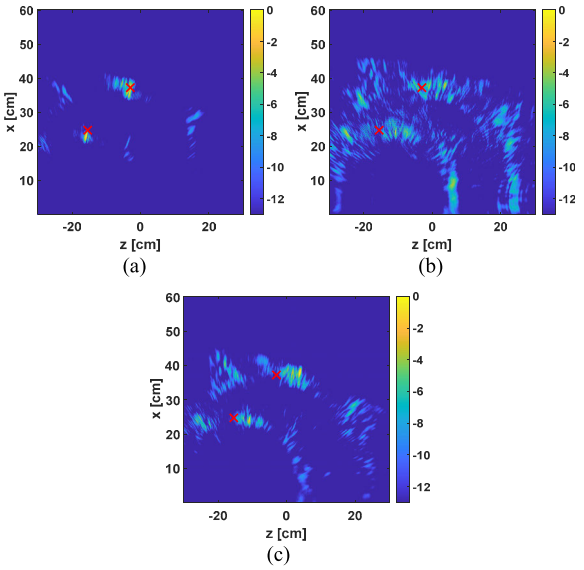

FIGURE 7. Reflectivity images using the velocity based ZVD information after two swings: (a) reference motion capture system, (b) IMU and (c) IMU+ZUPT.

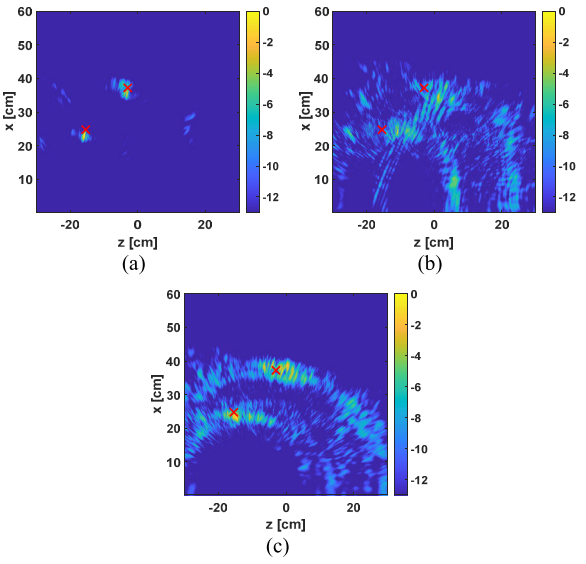

FIGURE 8. Reflectivity images using the acceleration based ZVD information after four swings: (a) reference motion capture system, (b) IMU and (c) IMU+ZUPT.

ZVD does not only modify the ZUPT + IMU reflectivity image, but also the other two (Figure 6(a, b) and 7(a, b)), since the swing defines the signals that have to be added coherently, as it was previously mentioned.

In these figures, the red crosses indicate the location of the two rods, which were determined using the reference motion capture system during the calibration stage. From the results, one can observe that the targets are clearly identified using the motion capture system and the IMU + ZUPT, whereas they are more blurred when using just the IMU system. For comparison purposes, Figure 6(d) shows the reflectivity image when considering only one radar position, noticing the

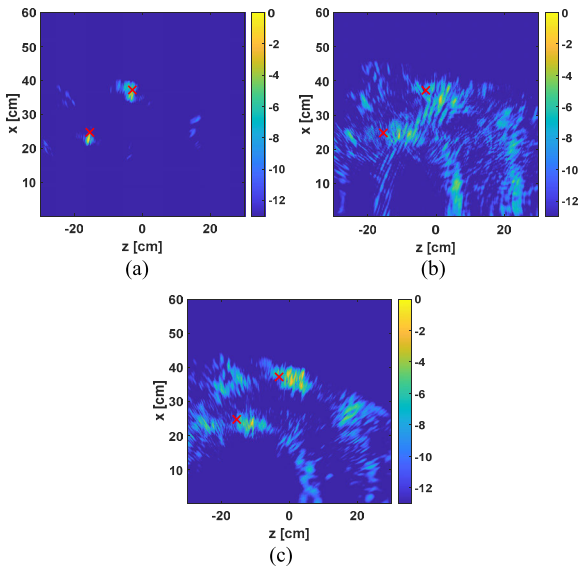

FIGURE 9. Reflectivity images using the velocity based ZVD information after 2 steps: (a) reference motion capture system, (b) IMU and (c) IMU+ZUPT.

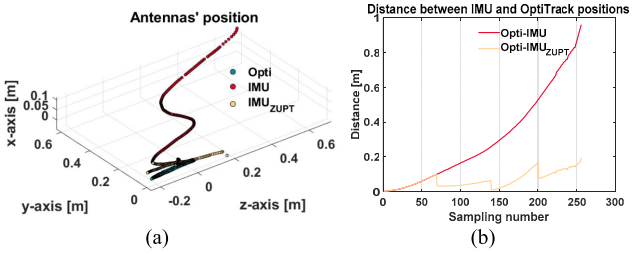

FIGURE 10. (a) Antennas' position and distance from reference system to IMU (Opti-IMU) and IMU+ZUPT (Opti-IMU$_{ZUPT}$), using the acceleration based ZVD.

lack of azimuth information. For the sake of compactness, this latter image will not be rendered in the subsequent figures as it is identical.

Figure 8 and 9 show the electromagnetic images after four swings. As one can notice, similar conclusions can be drawn. Although the best performance is achieved using the reference motion capture system, the results from the IMU+ZUPT image are also trustworthy. It is relevant to note that by increasing the number of swings, the image from the IMU is worsened, whereas the one from the IMU+ZUPT can be improved. Although the targets are clearly identified in the IMU+ZUPT, they are slightly shifted in the z-axis, probably due to a wrong estimation at the beginning of the swing when using the velocity based ZVD.

In Figures 10 and 11, the measurement positions are presented, as well as the difference, in terms of distance, between the position estimation of the reference system and the one computed using the IMU and IMU+ZUPT algorithms. As it can be noticed, an increasing error is observed when considering just the IMU data, whereas the increasing rate is significantly lower when applying the ZUPT algorithm, explaining the better quality of the reflectivity image.

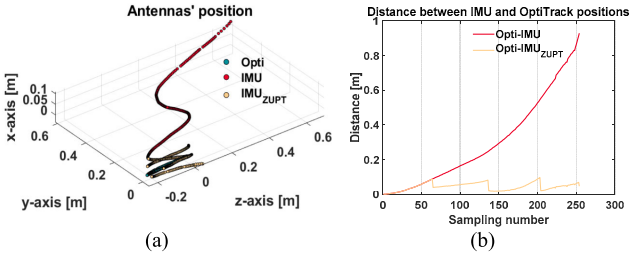

FIGURE 11. (a) Antennas' position and distance from reference system to IMU (Opti-IMU) and IMU+ZUPT (Opti-IMU$_{ZUPT}$), using the velocity based ZVD.

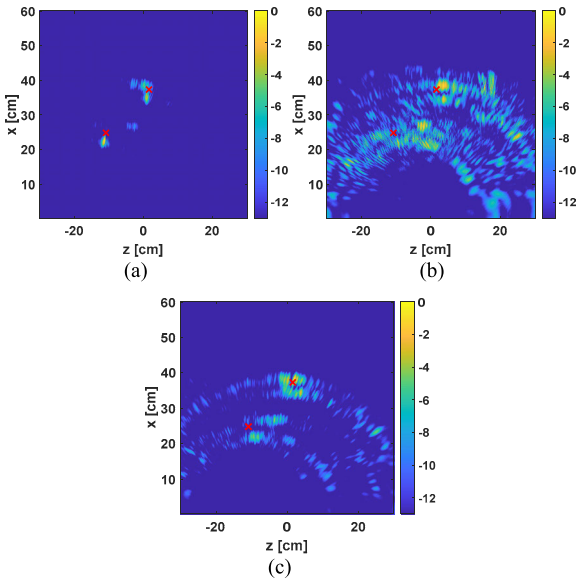

FIGURE 12. Reflectivity images using the acceleration based ZVD information with higher update rate after two swings: (a) reference motion capture system, (b) IMU and (c) IMU+ZUPT.

Using the same target, the second test comprises the parallel acquisition of positioning and radar data, which is then synchronized on the post-processing stage. This test will provide a faster update rate of the IMU information and hence, it may also reduce the positioning error or at least, slow down the quickly growing tendency. It should be noticed that the radar data cannot be acquired at faster rates, due to hardware and software limitations. Therefore, the new positioning system update rate is about 140 Hz, which is much higher than the previous one, 50 Hz, enabling a better tracking of the prototype.

In order to quantify the amount of energy around the target, the target-to-clutter ratio (TCR) is computed as follows [41]:

$$TCR = 10\,log\left(\frac{N_c \sum\limits_{(x,z)\epsilon A_t} |\rho(x,z)|^2}{N_t \sum\limits_{(x,z)\epsilon A_c} |\rho(x,z)|^2}\right), \tag{5}$$

where ρ is the reflectivity, A_t is the area enclosing the targets and A_c is the area outside the targets, and N_t and N_c are the number of pixels of A_t and A_c, respectively.

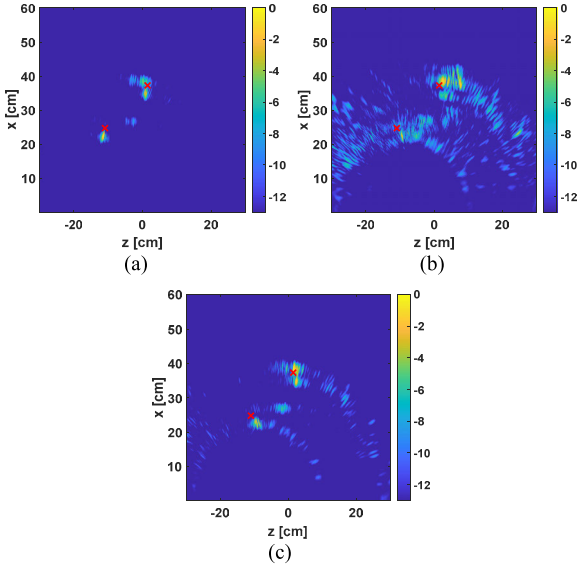

FIGURE 13. Reflectivity images using the velocity based ZVD information with higher update rate after two swings: (a) reference motion capture system, (b) IMU and (c) IMU+ZUPT.

TABLE 1. Target-to-clutter ratio at higher update rate.

Positioning subsystem	Arm swings	TCR (dB) (Acceleration ZVD)	TCR (dB) (Velocity ZVD)
Motion capture sys.	2	10.7	11.1
	4	10.6	10.9
IMU	2	5.6	6.8
	4	5.1	4.2
IMU+ZUPT	2	8.6	9.8
	4	7.8	8.4

FIGURE 14. Measurement set-up.

Figure 12 and 13 show the reflectivity images considering both the acceleration and velocity based ZVDs after two swings. As one can clearly observe, better results are achieved than for the case of updating the position at lower rates. This can be confirmed observing Table 1, where the TCR for both cases is presented, also including the results when four swings are considered. Once again, an improved performance is obtained when applying the ZUPT-based algorithm to the IMU data. In this case, it is not worth to consider more

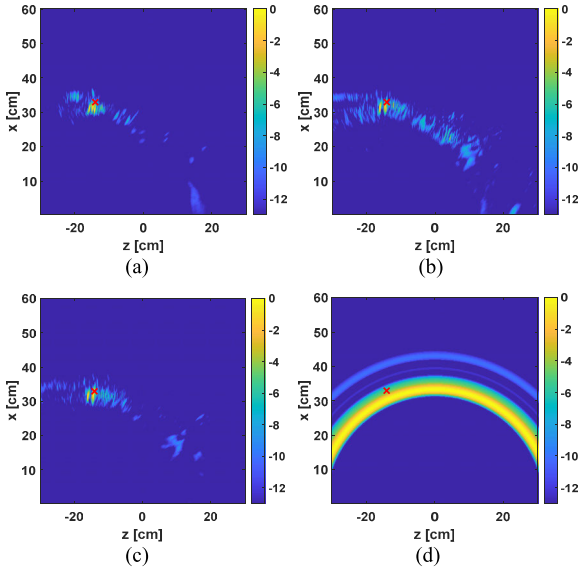

FIGURE 15. Reflectivity images using the acceleration based ZVD information with higher update rate after two swings: (a) reference motion capture system, (b) IMU and (c) IMU+ZUPT. (d) Reflectivity image considering only one radar position.

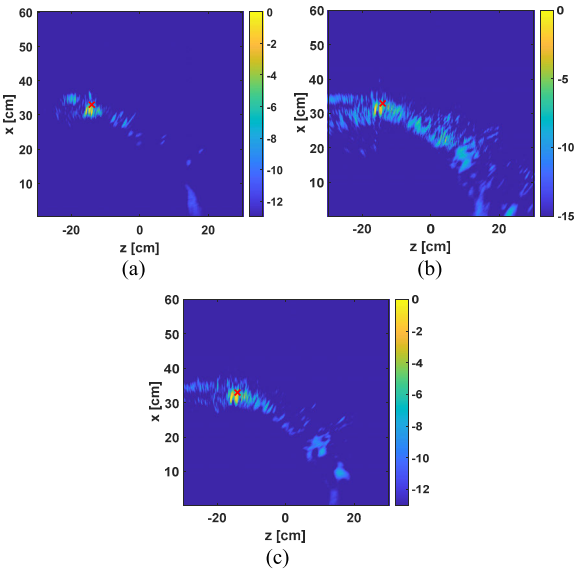

FIGURE 16. Reflectivity images using the velocity based ZVD information with higher update rate after two swings: (a) reference motion capture system, (b) IMU and (c) IMU+ZUPT.

than two swings, as the reflectivity images are not improved. Although this could seem counterintuitive, more swings will result in better TCR if the results between swings are consistent (e.g., there is no spatial offset between them). However, in the case of gathering the positioning information from the IMU and IMU+ZUPT, the coherence between arm swings is not perfect, so the results start degrading after a few swings.

In a second experiment, a different object, aiming at testing the versatility of the proposed system, is used. The new set-up is the one presented in Figure 14, which is identical to the previous one, but the target is modified. In this case just one wider target of 3.8 cm is considered.

TABLE 2. Target-to-clutter ratio (one target).

Positioning subsystem	Arm swings	TCR (dB) (Acceleration ZVD)	TCR (dB) (Velocity ZVD)
Motion capture sys.	2	12	12
	4	13	13.1
IMU	2	9.8	9.8
	4	8.5	8.4
IMU+ZUPT	2	12	12
	4	11.9	11.5

The reflectivity images are presented in Figure 15(a,b,c) and 16 and the TCR information is gathered in Table 2. It can be clearly observed that the target can be identified from the results using the reference motion capture system and the IMU+ZUPT algorithm, whereas when using only the IMU system the clutter increases. As in the previous case, the results considering just one radar position are presented in Figure 15(d).

IV. CONCLUSION

The possibility of enhancing the resolution of a wearable radar system by exploiting body movements has been presented in this paper. The approach has been illustrated for the case of considering movements in terms of arm swings. For this kind of movement, a prototype of handheld imager, comprising a mmWave radar and an inertial measurement unit (IMU), has been developed. The system has been designed using compact components showing the potential of implementing wearable devices, enabling easing its use for visually impaired people to detect objects and obstacles.

The study shows that a direct estimation of the trajectory from the acceleration integration is enough to focus the image energy at the position of the targets in contrast to the low resolution achieved from a single radar position. This improvement is achieved along the cross-range dimension. In the considered prototype, based on position tracking from IMU data, the resolution can be further improved if some enhancements are considered. For this purpose, two zero velocity techniques have been considered to correct the position estimation error computed from the IMU data and, hence, properly apply synthetic aperture radar (SAR) techniques to generate accurate electromagnetic images of the nearby environment. It should be mentioned that the IMU is a mean to achieve the main goal of this paper that is to show that compact mmWave radars can take advantage of the human movement to enhance their obstacle detection capabilities.

These techniques have been proved successful in detecting different targets, showing an accuracy similar to the one achieved when using a high accuracy external positioning system. Future research will focus on exploring other sensors to be integrated on the proposed system in order to improve the detection of the zero velocity as well as on the use of direct tracking systems (e.g. depth and tracking cameras) to handle arbitrary movements.

REFERENCES

[1] M. I. Skolnik, *Introduction to RADAR Systems*. New York, NY, USA: McGraw-Hill, 1980.

[2] B.-C. Wang, *Digital Signal Processing Techniques and Applications in Radar Image Processing*, vol. 91. Hoboken, NJ, USA: Wiley, 2008.

[3] G. Alvarez-Narciandi, M. Lopez-Portugues, F. Las-Heras, and J. Laviada, "Freehand, agile, and high-resolution imaging with compact mm-wave radar," *IEEE Access*, vol. 7, pp. 95516–95526, 2019, doi: 10.1109/ACCESS.2019.2929522.

[4] V. K. Kukkala, J. Tunnell, S. Pasricha, and T. Bradley, "Advanced driver-assistance systems: A path toward autonomous vehicles," *IEEE Consum. Electron. Mag.*, vol. 7, no. 5, pp. 18–25, Sep. 2018, doi: 10.1109/MCE.2018.2828440.

[5] S. Jardak, M.-S. Alouini, T. Kiuru, M. Metso, and S. Ahmed, "Compact mmWave FMCW radar: Implementation and performance analysis," *IEEE Aerosp. Electron. Syst. Mag.*, vol. 34, no. 2, pp. 36–44, Feb. 2019, doi: 10.1109/MAES.2019.180130.

[6] H. Aghasi and P. Heydari, "Millimeter-wave radars-on-chip enabling next-generation cyberphysical infrastructures," *IEEE Commun. Mag.*, vol. 58, no. 12, pp. 70–76, Dec. 2020, doi: 10.1109/MCOM.001.2000544.

[7] H. F. Álvarez, G. Álvarez-Narciandi, M. García-Fernández, J. Laviada, Y. Á. López, and F. L.-H. Andrés, "A portable electromagnetic system based on mm-wave radars and GNSS-RTK solutions for 3d scanning of large material piles," *Sensors*, vol. 21, no. 3, pp. 1–19, Feb. 2021, doi: 10.3390/s21030757.

[8] C. X. Lu, S. Rosa, P. Zhao, B. Wang, C. Chen, J. A. Stankovic, N. Trigoni, and A. Markham, "See through smoke: Robust indoor mapping with low-cost mmWave radar," in *Proc. MobiSys*, Jun. 2020, pp. 14–27, doi: 10.1145/3386901.3388945.

[9] L. Shao, J. Han, K. Pushmeet, and Z. Zhang, *Computer Vision and Machine Learning with RGB-D Sensors*. Cham, Switzerland: Springer, 2014.

[10] J. Guan, S. Madani, S. Jog, S. Gupta, and H. Hassanieh, "Through fog high-resolution imaging using millimeter wave radar," in *Proc. IEEE/CVF Conf. Comput. Vis. Pattern Recognit. (CVPR)*, Jun. 2020, pp. 11461–11470, doi: 10.1109/CVPR42600.2020.01148.

[11] W. Elmannai and K. Elleithy, "Sensor-based assistive devices for visually-impaired people: Current status, challenges, and future directions," *Sensors*, vol. 17, no. 3, p. 565, 2017, doi: 10.3390/s17030565.

[12] T. Kiuru, M. Metso, M. Utriainen, K. Metsävainio, H.-M. Jauhonen, R. Rajala, R. Savenius, M. Ström, T.-N. Jylhä, R. Juntunen, and J. Sylberg, "Assistive device for orientation and mobility of the visually impaired based on millimeter wave radar technology—Clinical investigation results," *Cogent Eng.*, vol. 5, no. 1, Jan. 2018, Art. no. 1450322, doi: 10.1080/23311916.2018.1450322.

[13] L. Scalise, V. M. Primiani, P. Russo, D. Shahu, V. Di Mattia, A. De Leo, and G. Cerri, "Experimental investigation of electromagnetic obstacle detection for visually impaired users: A comparison with ultrasonic sensing," *IEEE Trans. Instrum. Meas.*, vol. 61, no. 11, pp. 3047–3057, Nov. 2012, doi: 10.1109/TIM.2012.2202169.

[14] E. Cardillo, V. Di Mattia, G. Manfredi, P. Russo, A. De Leo, A. Caddemi, and G. Cerri, "An electromagnetic sensor prototype to assist visually impaired and blind people in autonomous walking," *IEEE Sensors J.*, vol. 18, no. 6, pp. 2568–2576, Mar. 2018, doi: 10.1109/JSEN.2018.2795046.

[15] K. Wang, R. Cheng, K. Yang, J. Bai, and N. Long, "Fusion of millimeter wave radar and RGB-depth sensors for assisted navigation of the visually impaired," *Proc. SPIE*, vol. 10800, Oct. 2018, Art. no. 1080006, doi: 10.1117/12.2324626.

[16] N. Long, K. Wang, R. Cheng, K. Yang, W. Hu, and J. Bai, "Assisting the visually impaired: Multitarget warning through millimeter wave radar and RGB-depth sensors," *J. Electron. Imag.*, vol. 28, no. 1, p. 1, Feb. 2019, doi: 10.1117/1.jei.28.1.013028.

[17] P. Kwiatkowski, T. Jaeschke, D. Starke, L. Piotrowsky, H. Deis, and N. Pohl, "A concept study for a radar-based navigation device with sector scan antenna for visually impaired people," in *IEEE MTT-S Int. Microw. Symp. Dig.*, May 2017, pp. 1–4, doi: 10.1109/IMBIOC.2017.7965796.

[18] F. Bovenga, "Special issue 'synthetic aperture radar (SAR) techniques and applications,"' *Sensors*, vol. 20, no. 7, p. 1851, Mar. 2020, doi: 10.3390/s20071851.

[19] J. C. Curlander and R. N. McDonough, *Synthetic Aperture Radar*, vol. 11. New York, NY, USA: Wiley, 1991.

[20] R. Mautz and S. Tilch, "Survey of optical indoor positioning systems," in *Proc. Int. Conf. Indoor Positioning Indoor Navigat.*, Sep. 2011, pp. 1–7, doi: 10.1109/IPIN.2011.6071925.

[21] S. S. Saab and Z. S. Nakad, "A standalone RFID indoor positioning system using passive tags," *IEEE Trans. Ind. Electron.*, vol. 58, no. 5, pp. 1961–1970, May 2011, doi: 10.1109/TIE.2010.2055774.

[22] D. Wells, N. Beck, A. Kleusberg, E. J. Krakiwsky, G. Lachapelle, R. B. Langley, K. P. Schwarz, J. M. Tranquilla, P. Vanicek, and D. Delikaraoglou, "Guide to GPS positioning," Dept. Geodesy Geomatics Eng., Univ. New Bnmswick, Fredericton, NB, Canada, Lect. Note 58, 1987.

[23] Y. López, G. Narciandi, and F. L.-H. Andrés, "Sensor network and inertial positioning hybridisation for indoor location and tracking applications," *Int. J. Sens. Netw.*, vol. 24, no. 4, pp. 242–252, Jan. 2017, doi: 10.1504/IJSNET.2017.085977.

[24] A. Yamashita, K. Sato, S. Sato, and K. Matsubayashi, "Pedestrian navigation system for visually impaired people using HoloLens and RFID," in *Proc. Conf. Technol. Appl. Artif. Intell. (TAAI)*, Dec. 2017, pp. 130–135, doi: 10.1109/TAAI.2017.9.

[25] G. Alvarez-Narciandi, J. Laviada, and F. Las-Heras, "Towards turning smartphones into mmWave scanners," *IEEE Access*, vol. 9, pp. 45147–45154, 2021, doi: 10.1109/ACCESS.2021.3067458.

[26] S. O. H. Madgwick, A. J. L. Harrison, and R. Vaidyanathan, "Estimation of IMU and MARG orientation using a gradient descent algorithm," in *Proc. IEEE Int. Conf. Rehabil. Robot.*, Jun. 2011, pp. 1–7, doi: 10.1109/ICORR.2011.5975346.

[27] R. Mahony, T. Hamel, and J.-M. Pflimlin, "Nonlinear complementary filters on the special orthogonal group," *IEEE Trans. Autom. Control*, vol. 53, no. 5, pp. 1203–1218, Jun. 2008, doi: 10.1109/TAC.2008.923738.

[28] X. Yun, E. R. Bachmann, and R. B. Mcghee, "A simplified quaternion-based algorithm for orientation estimation from earth gravity and magnetic field measurements," *IEEE Trans. Instrum. Meas.*, vol. 57, no. 3, pp. 638–650, Mar. 2008, doi: 10.1109/TIM.2007.911646.

[29] H. M. Schepers, H. F. J. M. Koopman, and P. H. Veltink, "Ambulatory assessment of ankle and foot dynamics," *IEEE Trans. Biomed. Eng.*, vol. 54, no. 5, pp. 895–902, May 2007, doi: 10.1109/TBME.2006.889769.

[30] A. Filippeschi, N. Schmitz, M. Miezal, G. Bleser, E. Ruffaldi, and D. Stricker, "Survey of motion tracking methods based on inertial sensors: A focus on upper limb human motion," *Sensors*, vol. 17, no. 6, p. 1257, Jun. 2017, doi: 10.3390/s17061257.

[31] M. Khedr and N. El-Sheimy, "A smartphone step counter using IMU and magnetometer for navigation and health monitoring applications," *Sensors*, vol. 17, no. 11, p. 2573, Nov. 2017, doi: 10.3390/s17112573.

[32] E. Foxlin, "Pedestrian tracking with shoe-mounted inertial sensors," *IEEE Comput. Graph. Appl.*, vol. 25, no. 6, pp. 38–46, Nov. 2005, doi: 10.1109/MCG.2005.140.

[33] I. Skog, P. Handel, J.-O. Nilsson, and J. Rantakokko, "Zero-velocity detection—An algorithm evaluation," *IEEE Trans. Biomed. Eng.*, vol. 57, no. 11, pp. 2657–2666, Nov. 2010, doi: 10.1109/TBME.2010.2060723.

[34] Z. Chen, X. Pan, M. Wu, S. Zhang, L. An, and M. Wang, "A novel adaptive zero-velocity detector for inertial pedestrian navigation based on optimal interval estimation," *IEEE Access*, vol. 8, pp. 191888–191900, 2020, doi: 10.1109/ACCESS.2020.3030975.

[35] N. Yu, Y. Li, X. Ma, Y. Wu, and R. Feng, "Comparison of pedestrian tracking methods based on foot- and waist-mounted inertial sensors and handheld smartphones," *IEEE Sensors J.*, vol. 19, no. 18, pp. 8160–8173, Sep. 2019, doi: 10.1109/JSEN.2019.2919721.

[36] M. S. Saadat, S. Sur, S. Nelakuditi, and P. Ramanathan, "MilliCam: Hand-held millimeter-wave imaging," in *Proc. 29th Int. Conf. Comput. Commun. Netw. (ICCCN)*, Aug. 2020, pp. 1–9, doi: 10.1109/ICCCN49398.2020.9209710.

[37] I. Nasr, R. Jungmaier, A. Baheti, D. Noppeney, J. S. Bal, M. Wojnowski, E. Karagozler, H. Raja, J. Lien, I. Poupyrev, and S. Trotta, "A highly integrated 60 GHz 6-channel transceiver with antenna in package for smart sensing and short-range communications," *IEEE J. Solid-State Circuits*, vol. 51, no. 9, pp. 2066–2076, Sep. 2016, doi: 10.1109/JSSC.2016.2585621.

[38] J. Lien, N. Gillian, M. E. Karagozler, P. Amihood, C. Schwesig, E. Olson, H. Raja, and I. Poupyrev, "Soli: Ubiquitous gesture sensing with millimeter wave radar," *ACM Trans. Graph.*, vol. 35, no. 4, p. 142, 2016, doi: 10.1145/2897824.2925953.

[39] *LPMS-CURS2: OEM Version 9-Axis Inertial Measurement Unit (IMU)/AHRS With USB, CAN Bus and UART Connectivity–LP-RESEARCH*. Accessed: May 11, 2021. [Online]. Available: https://lp-research.com/lpms-curs2/

[40] J.-O. Nilsson, I. Skog, P. Handel, and K. V. S. Hari, "Foot-mounted INS for everybody—An open-source embedded implementation," in *Proc. IEEE/ION Position, Location Navigat. Symp.*, Apr. 2012, pp. 140–145, doi: 10.1109/PLANS.2012.6236875.

[41] L. Liu, Q. Chen, Y. Han, H. Xu, J. Li, and B. Wang, "Improved clutter removal by robust principal component analysis for chaos through-wall imaging radar," *Electronics*, vol. 9, no. 1, p. 25, Dec. 2019, doi: 10.3390/electronics9010025.

HUMBERTO FERNÁNDEZ ÁLVAREZ was born in Oviedo, Asturias, Spain, in 1989. He received the M.S. degree in telecommunication engineering and the Ph.D. degree (Hons.) from the University of Oviedo, Asturias, Spain, in 2014 and 2019, respectively. In 2017, he was a Visiting Scholar with the Department of Mechanical, Electrical and Manufacturing Engineering, Loughborough University. He is currently working as a Researcher with the Signal Theory and Communications Research Group (TSC-UNIOVI). His research interests include metamaterials, metasurfaces (frequency selective surfaces, artificial magnetic conductors, and absorbers), antennas, electromagnetic propagation, computational electromagnetics, measurement techniques, radar technologies, and imaging techniques. He was granted by the Asturias Government for conducting his Ph.D. within the University of Oviedo in an area of signal theory and communications. He received the 2020 National Award to the Best Ph.D. Thesis on Telecommunication Engineering (category: satellite communication systems), the Extraordinary Ph.D. Prize from Oviedo University, the Best Final Degree Research Project Award from Cá tedra Telefó nica, in 2015, and a Research Contract from the University of Oviedo.

GUILLERMO ÁLVAREZ-NARCIANDI received the M.Sc. degree in telecommunication engineering and the Ph.D. degree from the University of Oviedo, Gijón, Spain, in 2016 and 2020, respectively. He was a Visiting Student with Stanford University, Stanford, CA, USA, in 2014, and a Visiting Scholar with the University of Pisa, Italy, in 2018, and the Institute of Electronics, Microelectronics and Nanotechnology (IEMN), University of Lille, France, in 2019. His research interests include radar systems and imaging techniques, antenna diagnosis and characterization systems, localization and attitude estimation systems, and RFID technology. He received the AMTA 2019 Student Paper Award (second place) and the Special Award to the Best Entrepreneurship Initiative in the XV Arquí medes National Contest for the development of a RFID-based location system, in 2017.

FERNANDO LAS-HERAS (Senior Member, IEEE) received the M.S. and Ph.D. degrees in telecommunication engineering from the Technical University of Madrid (UPM), in 1987 and 1990, respectively. From 1988 to 1990, he was a National Graduate Research Fellow, and from 1991 to 2000, he was an Associate Professor with the Department of Signal, Systems and Radio Communications, UPM. Since 2001, he has been heading the Signal Theory and Communications Research Group (TSC-UNIOVI), Department of Electrical Engineering, University of Oviedo. Since 2003, he has been a Full Professor with the University of Oviedo, where he was the Vice-Dean of telecommunication engineering with the Technical School of Engineering, Gijón, from 2004 to 2008. He was a Visiting Lecturer with the National University of Engineering, Peru, in 1996, a Visiting Researcher with Syracuse University, New York, in 2000, and a short-term Visiting Lecturer with ESIGELEC, France, from 2005 to 2011. From 2005 to 2015, he held the Telefónica Chair on "RF Technologies," "ICTs applied to Environment," and "ICTs and Smart cities" with the University of Oviedo. He has authored scientific articles in the areas of antennas, EM scattering, meta-materials, and inverse problems with application to antenna measurement (NF-FF, diagnostics, and holography), electromagnetic imaging (security and NDT) and localization, developing computational electromagnetics algorithms and technology on microwaves, millimeter wave, and THz frequency bands. He was a member of the Board of Director of the IEEE Spain Section, from 2012 to 2015, the Board of IEEE Microwaves and Antennas Propagation Chapter (AP03/MTT17), from 2016 to 2017, the Science, Technology and Innovation Council, Asturias, from 2010 to 2012, and the President of the Professional Association of Telecommunication Engineers, Asturias.

JAIME LAVIADA was born in Gijón, Spain. He received the M.S. degree in telecommunication engineering and the Ph.D. degree from the Universidad de Oviedo, Spain, in 2005 and 2010, respectively. In 2006, he joined the Signal Theory and Communications Research Group, Universidad de Oviedo, where he has been involved in multiple national and European projects as well as contracts with several companies. In 2015, he moved to the Antennas Group, Universidad Pública de Navarra, with a National Postdoctoral Fellowship collaborating in several applied research projects. Finally, he moved back to the Universidad de Oviedo, where he is currently an Associate Professor. In addition, he has been a Visiting Scholar with the Electromagnetics and Communications Laboratory, Pennsylvania State University, from 2007 to 2008, and with the Applied Microwave Non-Destructive Testing Laboratory, Missouri University of Science and Technology, in 2017. His research interests include numerical techniques applied to EM imaging, antenna measurements, method of moments, and antenna pattern synthesis.